Catalysis Today xxx (2015) xxx–xxx

Contents lists available at ScienceDirect

Catalysis Today

journal homepage: www.elsevier.com/locate/cattod

Change in reactivity of differently capped AuPd bimetallic nanoparticle catalysts for selective oxidation of aliphatic diols to hydroxycarboxylic acids in basic aqueous solution

Jaya Tuteja, Shun Nishimura, Kohki Ebitani *

School of Materials Science, Japan Advanced Institute of Science and Technology, 1-1 Asahidai, Nomi, Ishikawa 923-1292, Japan

ARTICLE INFO

Article history:
Received 2 July 2015
Received in revised form
15 September 2015
Accepted 22 September 2015
Available online xxx

Keywords:
Selective oxidation
ω-Hydroxycarboxylic acids
Capped AuPd bimetallic nanopaticles
Heterogeneous catalysts

ABSTRACT

N,N-Dimethyldodecylamine *N*-oxide (DDAO), PVP and PVA capped supported AuPd bimetallic nanoparticles (NPs) were prepared, and their catalytic activities were evaluated for the oxidation of 1,6-hexanediol (HDO) to 6-hydroxycaproic acid (HCA) using H_2O_2 in basic aqueous solution. Among three catalysts, DDAO capped AuPd bimetallic NPs catalysts exhibited superior selectivity for HCA formation than PVP and PVA capped catalysts. To explain the difference in the catalytic behavior, the catalysts were characterized thoroughly. XRD, TEM and STEM-HAADF-EDS studies were employed to identify the structure and morphology of capped AuPd-NPs, respectively. The chemical and electronic states were elucidated using XPS and XAS methods. The characterization data revealed that the capping agent significantly influences the electron density on metals and extent of alloying between Au and Pd metals. It was revealed that DDAO-capped catalyst induces appropriate negatively charged Au species with a few numbers of Au–Pd interfaces for the highly selective formation of HCA *via* HDO oxidation in basic aqueous media. Furthermore, other aliphatic diols, 1,7-heptanediol, 1,8-octanediol and 1,2-hexanediol, were also selectively oxidized on AuPd-DDAO catalysts toward the corresponding ω-hydroxycarboxylic acids in high yields.

1. Introduction

The selective oxidation of aliphatic diol to monohydroxycarboxylic acid is an important and a fundamental organic reaction (Scheme 1) [1–5]. A variety of reaction systems has been derived in traditional oxidation processes using homogeneous catalysts [6] or stoichiometric reagents such as chromates [7] and permanganates [8]. However, these methods are not environmentally sustainable due to generation of a large amount of toxic wastes [9]. Thus, the development of environmentally benign and clean oxidation reactions remains an important goal of chemical research [10,11].

From the viewpoint of green and sustainable chemistry, metallic nanoparticles (NPs) have received a great deal of attention in the last decade because of their properties and potential application in oxidation catalysis [12–14]. In order to improve chemical and physical properties of metal NPs for catalysis, the addition of second metal is often employed [15–17]. Combining the properties of associated two individual metal demonstrated many advantages in various catalytic reactions [18–21]. The bimetallic NPs systems have been noticed to improve the product selectivity, catalyst durability and the reaction kinetics [22,23]. The surpassing performance of bimetallic NPs has been commonly ascribed to "electronic effect" or "ensemble effect" [24–28]. The first affect could be accounted for modification in electronic structure *via* bimetallic interactions which alter the electron density of each metal. The second effect corresponds to the relative location of two metals on NP surface. Thus, the catalytic activity can be tuned by controlling the electronic properties and local structure of bimetallic NPs. For example, catalysis over Au-Pd bimetallic NPs has received the greater consideration among noble metals [19,25,29], because it exhibits a significant catalytic performance in comparison with those of monometallic Au or Pd NPs.

It is well-known that the metal composition, size and shape of NPs have notable influence on their catalytic properties. In addition, the surface capping agents (organics or polymers) which are generally used in the synthesis of NPs to keep the particles suspended [30], also influences the catalytic activity to a significant extent; for instance, DDAO has been discovered as an efficient capping agent inducing special catalytic properties which lead to high

* Corresponding author.
E-mail address: ebitani@jaist.ac.jp (K. Ebitani).

http://dx.doi.org/10.1016/j.cattod.2015.09.034
0920-5861/

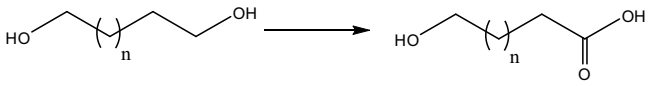

Scheme 1. Selective oxidation of aliphatic diol to mono-hydroxycarboxylic acid.

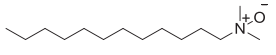

N,*N*-dimethyldodecylamine *N*-oxide (DDAO)

Poly(*N*-vinyl-2-pyrrolidone) (PVP)

Poly(vinyl alcohol) (PVA)

Fig. 1. Structure of capping agents used in this study.

selectivity of the product [31,32]. The development of colloidal synthesis has the ability to precisely tailor the structural characteristics (size, shape and distribution) usually by varying the amount of capping agent [33–35]. On the other hand, the choice of capping agent would significantly affect the electronic structures of bimetallic NPs along with the alterations in size- and/or shape-dependent properties of the NPs. Multiple research groups have explained the size-dependent properties of metal NPs but only few of them have discussed the influences from stabilizers [31,32,36–38]. Overall, the role of capping agent in catalytic activity and selectivity is not yet well-understood in spite of its importance in NP systems for studying heterogeneous catalysis.

In a very recent study, we have communicated a highly active and a selective *N*,*N*-dimethyldodecylamine *N*-oxide (DDAO, see Fig. 1)-capped AuPd bimetallic NPs supported on hydrotalcite (HT) surface as reusable heterogeneous catalyst for selective oxidation of 1,6-hexanediol (HDO) to 6-hydroxycaproic acid (HCA) using aqueous H_2O_2 under high-pH conditions (Scheme 2) [32]. The results suggested that the synergetic interactions between Au and Pd or Au–Pd nanoalloy center played crucial role in the excellent catalysis of AuPd-DDAO/HT for the selective oxidation of HDO toward HCA.

Our previous communication with supported AuPd-DDAO bimetallic NPs raises some additional interesting questions on the role of DDAO as capping agent. In this paper, in order to explore the influence of capping agent on the oxidation of HDO to HCA, the catalytic activity of DDAO-capped AuPd bimetallic catalyst was compared with those of AuPd capped with the two most widely used capping agents; poly(*N*-vinyl-2-pyrrolidone) (PVP) and poly(vinyl alcohol) (PVA) (Fig. 1).

The detailed characterizations of the catalysts have been carried out using XRD, TEM, XPS, XAS and STEM-HAADF-EDS techniques, and then the relationship between electronic structure and activity of AuPd nanostructures has been suggested. A suitable reaction mechanism and a role of capping agent are also proposed based on the experimental results. Finally, the catalysis of reusable and highly selective AuPd-DDAO/HT is verified for the selective oxidation of other long chain aliphatic diols like 1,7-heptanediol, 1,8-octanediol and 1,2-hexanediol.

2. Experimental

2.1. Chemicals

Hydrogen tetrachloroaurate (III) ($HAuCl_4{\cdot}4H_2O$), palladium chloride ($PdCl_2$), ethylene glycol (EG), adipic acid (AA), 1,6-hexanediol (HDO), 30% hydrogen peroxide (H_2O_2), 1-hexanol, hexanoic acid, potassium iodide (KI), chloroform ($CHCl_3$), poly(vinyl alcohol) (partially hydrolyzed) (PVA, Mw; 3500) and Au and Pd standards (ICP grade) were obtained from Wako Pure Chemical Industries, Ltd. Kanto Chemical Co., Inc. supplied sodium hydroxide (NaOH), potassium chloride (KCl), and sulfuric acid (H_2SO_4). *N*,*N*-Dimethyldodecylamine *N*-oxide (DDAO), 1,2-hexanediol, 2-hydroxyhexanoic acid, 1,7-heptanediol, pimelic acid, 1,8-octanediol, 8-hydroxy octanoic acid and suberic acid were purchased from Sigma–Aldrich, Co. LLC. Acros Organics provided 6-hydroxycaproic acid (HCA) and poly(*N*-vinyl-2-pyrrolidone) (PVP, K29-32, Mw; 58,000). Melatonin and hydrotalcite (HT, Mg/Al = 5.4) was obtained from TCI Chemicals Pvt. Ltd. and Tomita Pharmaceuticals Co. Ltd., respectively.

2.2. Catalyst preparation

Capped AuPd-X/HT catalysts have been synthesized as reported in the literatures [32,39,40] with some modifications. In a typical synthesis, an aqueous solution (50 mL) of $HAuCl_4{\cdot}4H_2O$ (0.04 mmol) and $PdCl_2$ (0.06 mmol) including KCl (0.18 mmol) were mixed with DDAO, PVP or PVA and stirred for 5 min at room temperature. Thereafter, EG (50 mL) was added into the aqueous mixture and again stirred for 5 min at room temperature, then the obtained mixture was refluxed for 2 h at 413 K, followed by addition of HT (1.0 g) into the formed colloidal dispersion to stabilize the formed AuPd-X NPs onto the surface of HT. The resultant mixture was stirred again for 1 h at 413 K. The obtained precipitates were cooled, filtered, washed and dried *in vacuo* overnight.

2.3. Catalytic testing

All experiments to test the catalytic activity were performed in a Schlenk tube (50 mL vol.) attached to a condenser. The catalytic activity was evaluated for HDO oxidation in basic aqueous media with H_2O_2 as oxidant to obtain HCA. In a typical reaction procedure, aliphatic diol (0.5 mmol) and catalyst (25 mg) were weighed and dispersed in deionized water (3.5 mL) in a Schenk tube. 30% H_2O_2 (0.75 mL) and 0.5 M NaOH (0.75 mL) were added to the above mixture, and then the Schlenk tube was mounted on a preheated oil bath at 353 K. The mixture was allowed to react for various time intervals with continuous magnetic stirring (500 rpm). After the reaction, a part of the resultant solution was diluted 20 times with an aqueous H_2SO_4 (10 mM) solution, and the catalyst was filtered off using a 0.20 μm filter (Milex®-LG). The obtained filtrate was analyzed by high performance liquid chromatography (HPLC, WATERS 600) using an Aminex HPX-87H column (Bio-Rad Laboratories, Inc.) attached to a refractive index detector. An aqueous 10 mM H_2SO_4 solution (eluent) was run through the column (maintained at 323 K) at a flow rate of 0.5 mL min^{-1}. The conversion and yield(s) were determined with a calibration curve method using commercial products.

2.4. Product isolation

The catalyst was separated from the reaction mixture *via* centrifugation followed by filtration using a 0.20 μm filter (Milex®-LG). The obtained mixture was acidified till pH = 1–2 by adding aq. H_2SO_4 drop wise. The compound was extracted with $CHCl_3$ (four times). The combined organic layers were condensed under reduced pressure to obtain product. The product was dissolved in $CDCl_3$ and subjected to NMR spectroscopy (Bruker BioSpin Inc. AVANCE III) for identification of product.

2.5. Characterization

Crystal structure was analyzed by powder X-ray diffraction (XRD) with a SmartLab (Rigaku Co.) using a Cu Kα radiation (λ = 0.154 nm) at 40 kV and 30 mA in the range of 2θ = 4–80°.

Please cite this article in press as: J. Tuteja, et al., Change in reactivity of differently capped AuPd bimetallic nanoparticle catalysts for selective oxidation of aliphatic diols to hydroxycarboxylic acids in basic aqueous solution, Catal. Today (2015), http://dx.doi.org/10.1016/j.cattod.2015.09.034

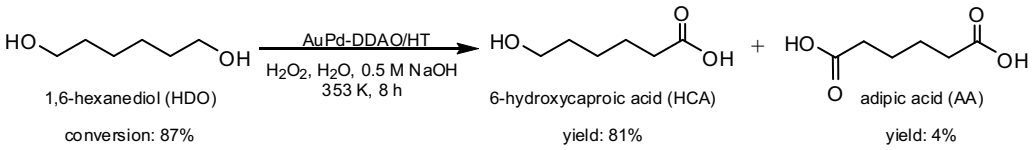

Scheme 2. Selective oxidation of 1,6-hexanediol (HDO) to 6-hydroxycaproic acid (HCA).

Ultraviolet–visible (UV–vis) spectrum was obtained by U-3900H (Hitachi, Ltd.) with a diffuse reflection method (integration sphere mode), and transformed by Kubelka–Munk (K-M) function. For inductively coupled plasma atomic emission spectroscopy (ICP-AES) analysis, an ICPS-7000 ver. 2 (Shimadzu Co.) was employed to quantify the real Au and Pd amount loaded over HT. Contents of metal (Au and/or Pd) in the catalyst and/or the reaction medium were estimated by a calibration curve method with commercial metal standards. An H-7100 (Hitachi, Ltd.) operating at 100 kV was utilized to acquire the morphology of catalyst by a transmission electron microscopy (TEM) image. High angle annular dark-field scanning TEM (HAADF-STEM) images with energy dispersive X-ray spectrometry (EDS) analysis were obtained with a JEOL-JEMARM200F operating at 200 kV. The samples for TEM measurements were dispersed in ethanol, and the supernatant liquid was dropped onto a carbon-coated copper grid before drying *in vacuo* overnight. The electronic states of capped AuPd NPs were analyzed by X-ray photoelectron spectroscopy (XPS) conducted on an AXIS-ULTRA DLD spectrometer system (Shimadzu Co. and Kratos Analytical Ltd.) using an Al target at 15 kV and 10 mA in an energy range of 0–1200 eV. The binding energies were calibrated with the C 1s level (284.5 eV) as an internal standard reference. The samples for X-ray absorption spectroscopy (XAS) study were pressed into a pellet and measured in transmission or fluorescence mode. XAS was performed at the BL-9C (Au L_{III}-edge) and the BL-9A (Pd L_{III}-edge) of Photon Factory at High Energy Accelerator Research Organization (KEK-PF), Tsukuba, Japan, under the Proposal No. 2013G586. The BL01B1 in the SPring-8 with the approval of the Japan Synchrotron Radiation Research Institute (JASRI) (Nos. 2014B1036 and 2014B1472) was also used for Pd K-edge XAS studies. Data analysis was performed with the use of the software package REX2000. After the $\chi(k)$ function was extracted from the extended X-ray absorption fine structure (EXAFS) data, Fourier transformation (FT) was performed on the k^3-weighted data in the ranges of $k = 3.0–13.0$ Å^{-1} and $k = 3.0–12.5$ Å^{-1} for the Au L_{III}-edge and Pd K-edge EXAFS, respectively.

3. Results and discussion

3.1. Catalytic activity of AuPd catalysts with different capping agents

Table 1 demonstrates the differences in the reactivity of AuPd-X/HT (where X is the name of capping agents; *i.e.* DDAO, PVP or PVA) catalysts for the oxidation of HDO to HCA using H_2O_2 in an aqueous NaOH solution. All three catalysts were found to be highly active for converting HDO (>90% conversion), however, selectivity for HCA was seen to be influenced with the kind of capping agent used. For instance, about 65% HCA selectivity was obtained with PVP and PVA capping agents (Table 1, entries 1 and 2) whereas 93% HCA selectivity with DDAO capped AuPd bimetallic catalyst was achieved (Table 1, entry 3). AA was formed as a major by-product with yields >20% for PVP and PVA capped catalysts.

Table 1 also depicts the actual amount of metal loading on HT by ICP-AES measurements and the average particle size of bimetallic NPs observed by TEM. Similar metal loadings on HT surface were noticed with PVP and DDAO capped catalysts complementing the theoretical metal ratios of Au/Pd = 40/60. When PVA was used as a capping agent, however, lower metal loading of Au and Pd on HT was observed. In spite of low metal loading in PVA capped catalyst, an efficient catalytic activity for HDO conversion (90%) was observed.

The TEM images showed that the NPs were well-dispersed on heterogeneous surface and the capping agent influenced on the average particle size and their distribution (see Supplementary data, Figure S1). The mean particle size of the capped AuPd bimetallic catalysts were observed in the range of 2.8–4.2 nm, where PVP afforded the smallest AuPd NPs (2.8 nm) and DDAO forming the largest NPs (4.2 nm). PVA had an intermediate particle size of 3.5 nm for AuPd NPs. It is hard to correlate the catalytic activity with the metal loading and the average particle size of these AuPd catalysts, and thereby the progress of the reaction was studied to throw light on observed behaviors.

The time course profiles of the HDO oxidation on AuPd-X/HT catalysts are plotted in Fig. 2. The results indicated that the rate of oxidation of HDO varied with the capping agents. For DDAO and PVA capped catalysts, a steady increase in HDO conversion was seen with the increase in time till 8 h (Fig. 2(A)). While with PVP as capping agent, the HDO conversion rapidly shot up to 72% in 2 h of the reaction, and in the next 6 h only about 20% increment was observed. An interesting pattern for yields of products was seen in contrast to the HDO conversion over AuPd-X/HT catalysts (Fig. 2(B) and (C)). HCA and AA were observed as the only two products formed under present reaction conditions. For instance, DDAO capped catalysts resulted into a continuous increase in HCA yield with negligible formation of AA. In the case of PVA capped catalysts, a continuous increase in the yields of HCA and AA was observed to afford HCA as a major product. On the other hands, 47% of HCA yield was obtained in 2 h over PVP capped catalyst while only about 10% increase in HCA yield was noticed for another 6 h, and the yield of AA increased up to 30% in 8 h. It should be noted that we could not observe any aldehyde or other intermediates, whereas the transformation of alcohol to acid generally occurs *via* aldehyde [41].

Considering the time courses of the HDO oxidation, two pathways can be proposed: (1) both the primary hydroxyl groups of HDO have been oxidized simultaneously, and (2) the hydroxyl groups are oxidized one after another; *i.e.* consequential reaction such as HDO to HCA, and then HCA to AA. Thus, to further certify the formation of AA is from HCA or HDO itself, the oxidation of HCA, the expected intermediate, on AuPd-X/HT catalysts was performed under the same reaction conditions (Figure S2). It was found that the further oxidation of HCA to AA was the fastest for PVP (58% HCA conversion), moderate for PVA (43% HCA conversion), and the slowest for DDAO (25% HCA conversion) capped catalysts, hence validating that the consequential oxidation of HDO as shown in Scheme 3, and the lowest ability of the AuPd-DDAO/HT catalyst for the oxidation of HCA into AA. This might explain the highest HCA selectivity of the AuPd-DDAO/HT catalyst in the HDO oxidation (Table 1).

In order to find out the reason for such a different activity in the oxidation reaction, the capped AuPd bimetallic catalysts were thoroughly characterized by various instrumental techniques as follows.

Please cite this article in press as: J. Tuteja, et al., Change in reactivity of differently capped AuPd bimetallic nanoparticle catalysts for selective oxidation of aliphatic diols to hydroxycarboxylic acids in basic aqueous solution, Catal. Today (2015), http://dx.doi.org/10.1016/j.cattod.2015.09.034

Table 1
Selective oxidation of HDO to HCA over AuPd-**X**/HT catalysts.[a]

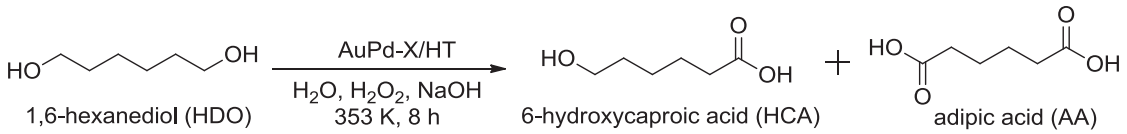

Entry	Catalyst	Conv./%[b]	Yield (sel.)/%[b]		Metal Loading[c]/mmol g^{-1}		Metal Particle Size[d]/nm
		HDO	HCA	AA	Au	Pd	
1	AuPd-PVP/HT	94	58 (62)	29 (31)	0.037	0.057	2.8
2	AuPd-PVA/HT	90	61 (68)	19 (21)	0.012	0.021	3.5
3	AuPd-DDAO/HT	87	81 (93)	4 (5)	0.034	0.056	4.2

[a] Reaction Conditions: HDO (0.5 mmol), catalyst (25 mg), 30% H_2O_2 (0.75 mL), 0.5 M NaOH (0.75 mL), H_2O (3.5 mL), 353 K, 8 h.
[b] Analysed by HPLC.
[c] Analysed by ICP-AES.
[d] Determined from TEM.

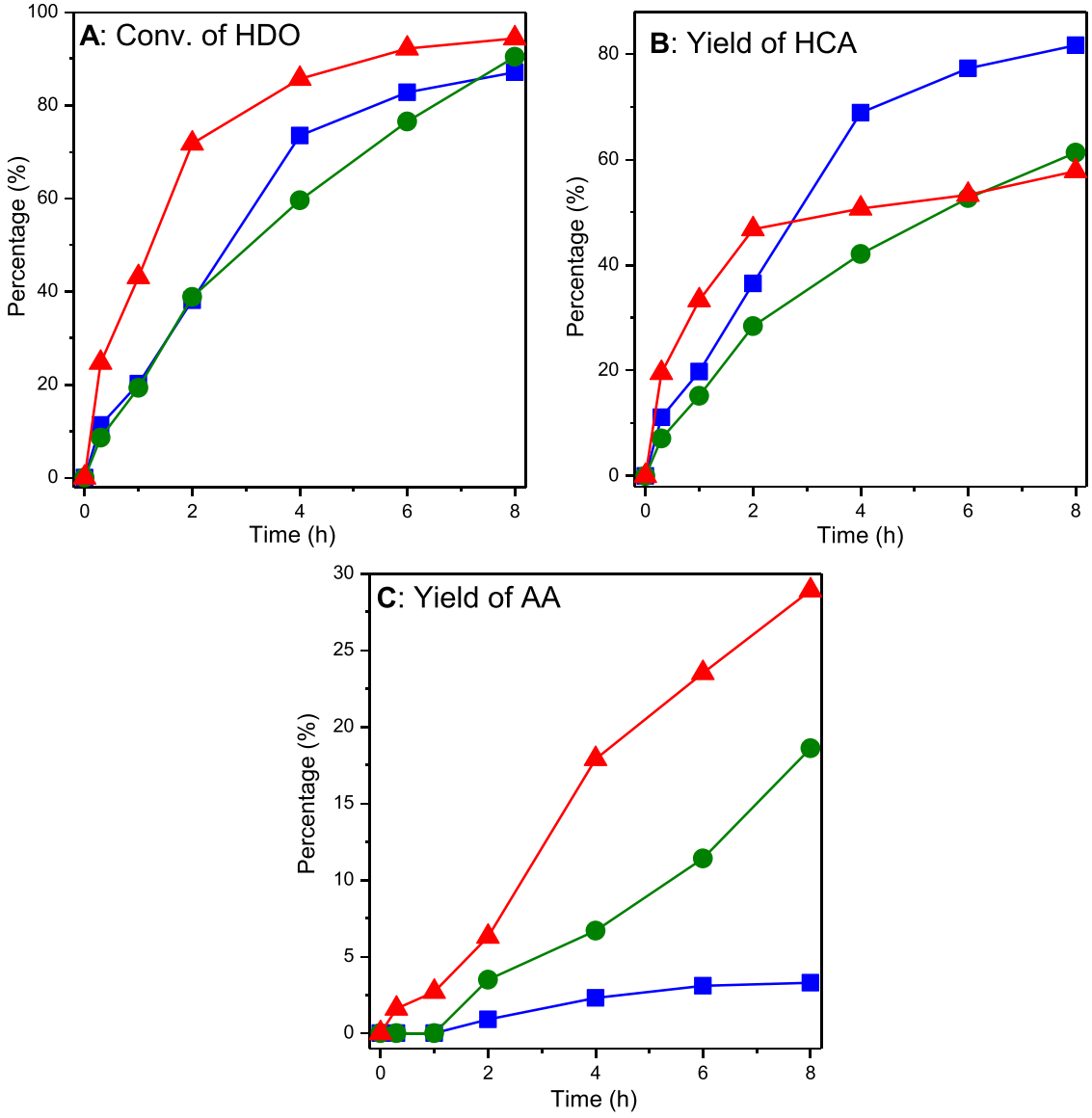

Fig. 2. Time course for selective oxidation of HDO over AuPd-X/HT, where X is PVP (▲), PVA (●) and DDAO (■). (A) Conversion of HDO, (B) Yield of HCA and (C) Yield of AA. *Reaction Conditions*: HDO (0.5 mmol), AuPd-X/HT (25 mg), H_2O (3.5 mL), 0.5 M NaOH (0.75 mL), 30% H_2O_2 (6 mmol), 353 K.

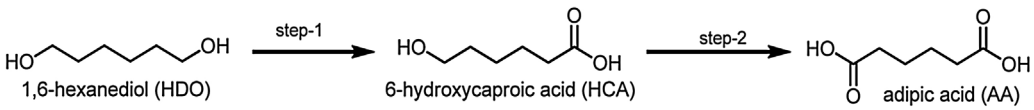

Scheme 3. Reaction pathway for HDO oxidation.

Please cite this article in press as: J. Tuteja, et al., Change in reactivity of differently capped AuPd bimetallic nanoparticle catalysts for selective oxidation of aliphatic diols to hydroxycarboxylic acids in basic aqueous solution, Catal. Today (2015), http://dx.doi.org/10.1016/j.cattod.2015.09.034

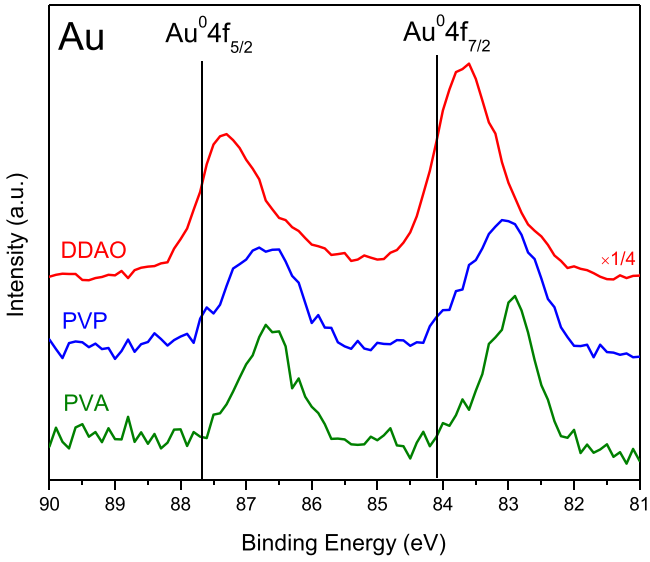

Fig. 3. Au 4f XPS spectra of AuPd-X NPs.

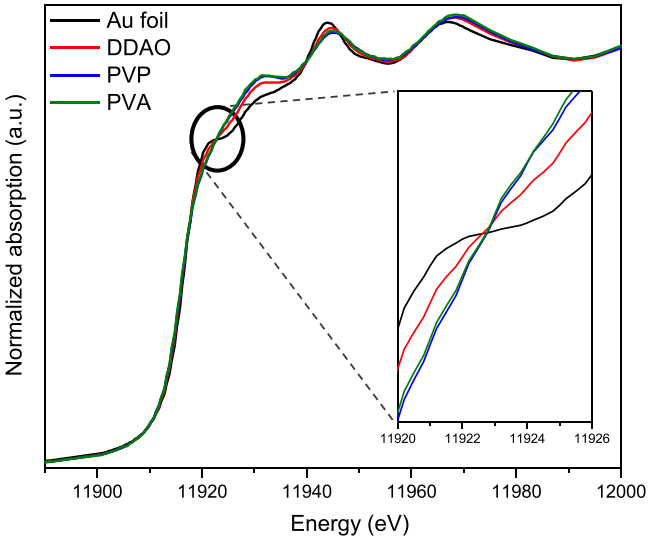

Fig. 4. Au L_{III}-edge XANES of AuPd-X/HT catalysts.

3.2. UV–vis spectrum and XRD pattern analyses

UV–vis spectrum was measured for supported capped AuPd bimetallic NPs and presented in Figure S3. From the literature, it is known that Au NPs shows a characteristic surface plasmon resonance (SPR) peak around 520 nm while Pd NPs does not show such absorption around here [42–46]. It was seen that the SPR band of the Au was completely damped in the supported capped AuPd bimetallic NPs (Figure S3). Therefore, the formation of Au–Pd bimetallic alloy NPs was suggested rather than separated monometallic Au and Pd NPs.

XRD patterns of capped AuPd bimetallic NPs (Figure S4) were monitored to verify the formation of Au–Pd bimetallic alloy NPs. The Au–Pd bimetallic NPs showed a broad band at around $2\theta = 38–39^\circ$ which is somewhat closer to the mean value of Pd(1 1 1) plane (40.06°) and Au(1 1 1) plane (38.19°) reflecting AuPd alloy formation [43–46]. The (1 1 1) diffraction signals for *fcc* structure were clearly visible in the case of DDAO capped NPs, while such features were not so clear in the case of PVP and PVA. The difference in XRD diffraction signal and intensity indicated that the extent of Au–Pd alloying is significant when NPs were synthesized with PVP and PVA as compared to DDAO as capping agent.

3.3. XPS analysis

XPS helps us to determine the surface composition and electronic properties of capped AuPd-X NPs. In general, the change in the core level binding energy (BE) as compared to pure metal is a strong indication of alloy formation because of charge transfer between metals. Fig. 3 shows the Au 4f XPS spectra of AuPd-X NPs. In AuPd bimetallic NPs system, it is more advantageous to specify the chemical state with the Au $4f_{7/2}$ peak because of the overlapping of core level of Au(0) $4f_{5/2}$ (87.7 eV) with Pd(0) 4s (88.2 eV) [47,48]. A significant negative shift (or shift to lower BE) for the Au 4f peaks of AuPd-X NPs was observed as compared to bulk Au(0) 4f. The negative shift in BE of Au $4f_{7/2}$ electrons for AuPd-X NPs was 1.2, 1.0 and 0.5 eV for PVA, PVP and DDAO capped AuPd bimetallic NPs in comparison to bulk Au $4f_{7/2}$. Such negative BE shift in the Au 4f peak for capped AuPd bimetallic catalysts has been reported exclusively in literatures [47–50], and attributed to charge transfer effects either from Pd or from capping agents to Au [49]. Here, we propose that the two major factors could be responsible for the observed difference in BE of Au 4f electrons for AuPd-X NPs as follows: (a) the difference in number of Au–Pd heterometallic bond (b) the difference in electron donation from their respective capping agents.

For AuPd-X NPs, where Au 4f showed much different electronic properties for different capping agents used, not significant information could be extracted from XPS spectra of Pd 3d (Figure S5) because of low intensity and overlapping peak in Pd 3d with Au $4d_{5/2}$ [39]. The observed BEs at 335.0 and 340.1 eV were assigned to Pd(0) $3d_{5/2}$ and $3d_{3/2}$, respectively, and it was noticed that Pd 3d XPS spectra of all three capped AuPd bimetallic NPs corresponds to Pd(0).

The information from the above XRD and XPS observations infer that there is a difference in the extent of alloying between two metals and electronic state of Au species in AuPd-X NPs.

3.4. X-ray absorption spectroscopy analysis

To get more information on the electronic effect and nanostructure caused by capping agents and its correlation with the catalytic activity, the XAS spectra were measured for Au-L_{III} and Pd-L_{III} and Pd-K edge for AuPd-X/HT catalysts and qualitatively compared to reference materials like foil and oxides.

3.4.1. XANES studies in Au and Pd L_{III}-edges

The Au L_{III}-edge probes the transition of 2p electrons to the 5d orbitals; the X-ray absorption near-edge structure (XANES) spectra of the Au L_{III}-edge of AuPd-X/HT are shown in Fig. 4. For all three bimetallic AuPd catalysts, a decrease in the white line (WL) intensity which is the first feature after the edge jump around 11,921 eV was observed, corresponding to the possibility of electron transition from 2p to 5d state in Au L_{III}-edge case. In other words, the decrease in WL intensity is observed for increase in the d-electron density of Au, which might possibly be due to electron transfer from Pd into 5d Au orbitals *via* Au–Pd alloying [51].

The inset image of Fig. 4 clearly shows a more electronegative Au species in case of PVP and PVA capped catalysts as compared to DDAO capped catalysts, lower intensities of these in WL area than DDAO, indicating more prominent Au–Pd alloying in case of PVP and PVA. Another important feature at the Au-L_{III} edge was the lower intensity of the second band (11,932 eV) with DDAO capped catalysts opposed to that of PVP and PVA capped ones. This feature again signified the lower mixing of the Au and Pd metals in DDAO capped catalyst.

Please cite this article in press as: J. Tuteja, et al., Change in reactivity of differently capped AuPd bimetallic nanoparticle catalysts for selective oxidation of aliphatic diols to hydroxycarboxylic acids in basic aqueous solution, Catal. Today (2015), http://dx.doi.org/10.1016/j.cattod.2015.09.034

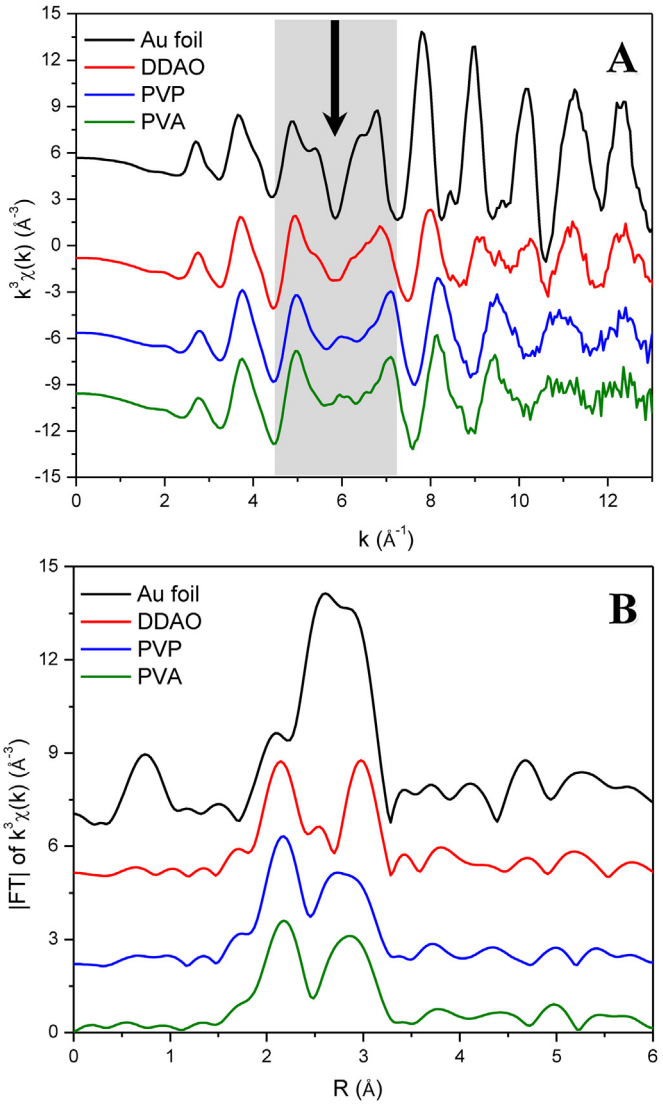

Fig. 5. Au L_{III}-edge (A) k^3-weighted EXAFS and (B) FT spectra of AuPd-X/HT catalysts.

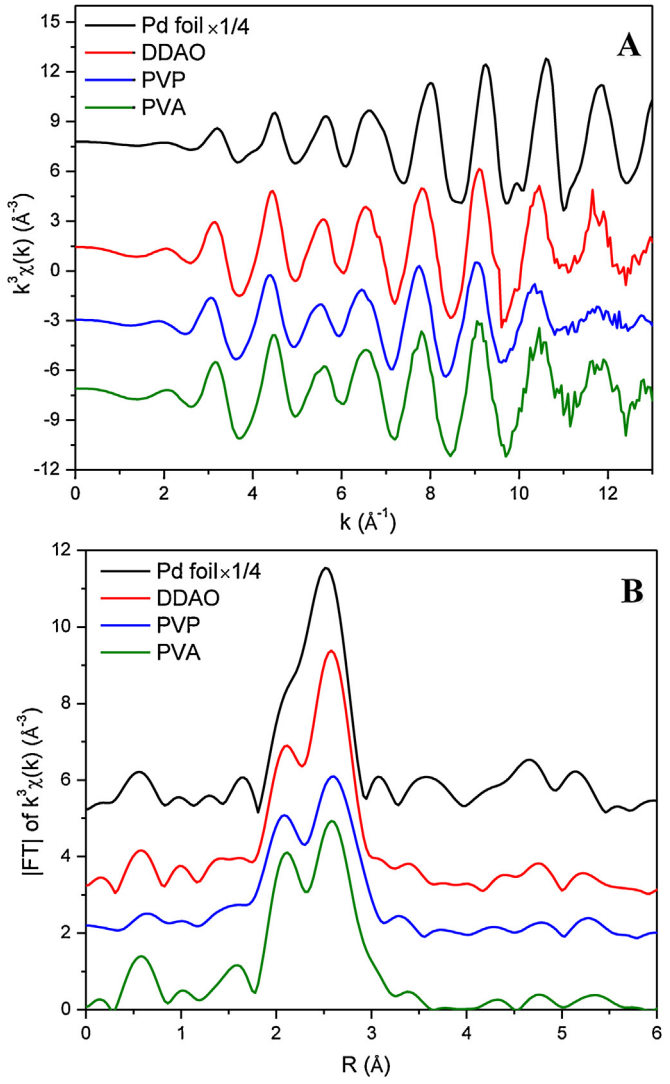

Fig. 6. Pd K-edge (A) k^3-weighted EXAFS and (B) FT spectra for AuPd-X/HT catalysts.

The Pd L_{III}-edge XANES spectra are shown in Figure S6. A significant decrease in WL intensity was seen from PVA > PVP > DDAO capped catalysts. The less intense WL for DDAO capped catalyst indicated the presence of more 4d-electrons in Pd [50], because the WL intensity is attributed from the transition from 2p to 4d state in Pd L_{III}-edge case. Similarly, above Au L_{III}-edge data suggested the lowest electronegativity of Au for DDAO capped catalysts among the three. Combining the results from both Au and Pd L_{III}-edge XANES suggested the lesser electronic interactions between Au and Pd metals (or low extent of Au–Pd alloying) when bimetallic NPs were synthesized with DDAO in contrast of PVP and PVA as capping agent.

3.4.2. FT and EXAFS studies in Au L_{III}-edge and Pd K-edge

Fig. 5 shows (A) the k^3-weighted EXAFS and (B) FT of EXAFS of the catalysts and Au foil in Au L_{III}-edge XAS. Some interesting features were seen in the EXAFS oscillation patterns of catalysts compared to that of Au foil. Fig. 5(A) shows that PVP and PVA capped catalysts exhibited quite different oscillation pattern to that of Au foil. For example, a clear diminshment of doublet character was seen in the region of 5–7 Å^{-1}, and another siginificant feature was the shift in oscillation waves. On contrary, no significant shift in the periodicity of the EXAFS wave was observed for DDAO capped catalysts. The diminishment of doublet character in the range of 5–7 Å^{-1} for AuPd bimetallic catalysts in contrast to Au foil is attributed to increase in neighboring Pd atoms in Au atoms, resulting in the formation of Au–Pd bonds [46]. The absence of any shift in the oscillation peaks for AuPd-DDAO/HT catalyst and partial diminishment of doublet peak (in the region of 5–7 Å^{-1}) suggests that the extent of alloying between the two metals is very low.

The FT of Au L_{III}-edge EXAFS spectra (Fig. 5(B)) for all catalysts exhibited sharp features in the region of 1.5–3.5 Å due to the first shell backscatter contributions [52]. For all the AuPd-X/HT catalysts, an intense doublet peak was seen in contrast to the Au foil (reference), indicating the occurrence of Au—Pd bond formation. The shift in the peak position of catalysts to 2.2 Å in reference to Au foil 2.6 Å reflected the significant contribution from backscattering of Au—Pd. Comparing the FT spectra of catalyst within themselves revealed that the splitting pattern in the range of 1.5–3.5 Å was quite different for DDAO from PVP and PVA capped catalysts. This splitting of the peak mainly arises from the interference between the EXAFS oscillations of the Au—Au and Au—Pd bonds [53]. The DDAO capped catalyst exhibits less intense doublets than the PVP and PVA capped catalysts, which supports the formation of less Au—Pd bonds in DDAO capped catalysts. Thus, the results from Au L_{III}-edge EXAFS study can be summarized as, the less intense splitting and similar EXAFS oscillation patterns of DDAO capped catalyst

Please cite this article in press as: J. Tuteja, et al., Change in reactivity of differently capped AuPd bimetallic nanoparticle catalysts for selective oxidation of aliphatic diols to hydroxycarboxylic acids in basic aqueous solution, Catal. Today (2015), http://dx.doi.org/10.1016/j.cattod.2015.09.034

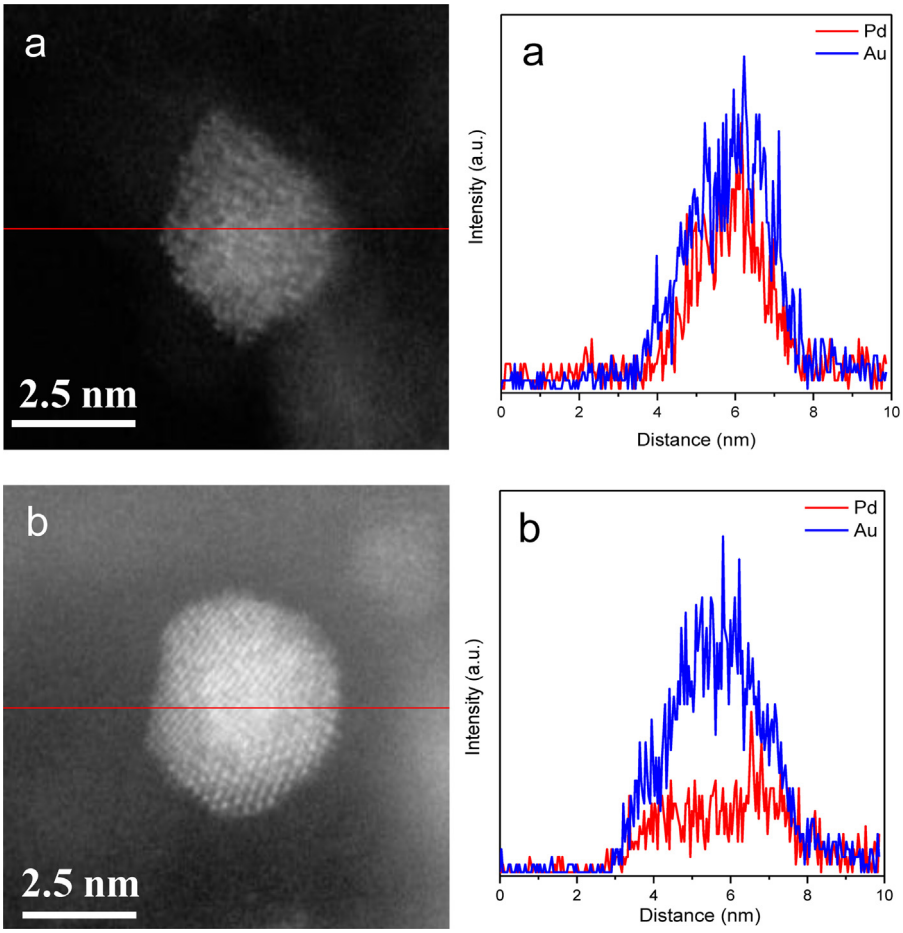

Fig. 7. STEM-EDS elemental line mapping of (a) AuPd-PVA/HT and (b) AuPd-DDAO/HT.

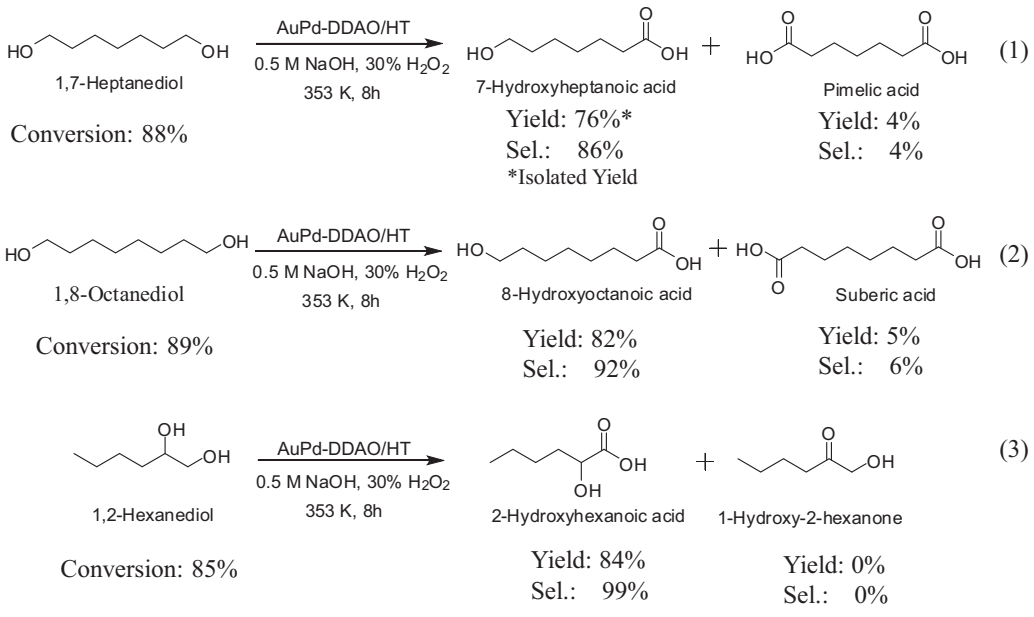

Fig. 8. AuPd-DDAO/HT-catalyzed selective oxidation of other aliphatic diols.

hints that the extent of alloying between Au and Pd is very low. On contrary, the extent of alloying is high when bimetallic NPs are capped with PVP or PVA.

To get additional information, we also studied the EXAFS at Pd K-edge. The Pd K-edge *k*-space EXAFS had very similar patterns for all the AuPd bimetallic catalysts and the reference Pd foil (Fig. 6(A)). Whereas, some alteration have been observed in the FT of Pd K-edge EXAFS spectra for catalysts as compared to Pd foil in Fig. 6(B). Similarly to FT of Au L_{III}-edge, in Pd K-edge also splitting occurs in the region of 1.7–3.3 Å which again confirms the formation of Au–Pd

Please cite this article in press as: J. Tuteja, et al., Change in reactivity of differently capped AuPd bimetallic nanoparticle catalysts for selective oxidation of aliphatic diols to hydroxycarboxylic acids in basic aqueous solution, Catal. Today (2015), http://dx.doi.org/10.1016/j.cattod.2015.09.034

random alloy in bimetallic capped catalysts. The intensification of doublet in case of PVP and PVA capped adds on to the previous suggestion that the extent of alloying between two metals is low in DDAO and high in case of PVP and PVA capped catalysts.

3.5. HAADF-STEM study with EDS analysis

HAADF-STEM analysis as shown in Fig. 7 further supports a structure of capped-bimetallic AuPd NPs on HT surface (see Figures S7–S9). Inspection of the elemental mapping image shows the uniform distribution and homogenous mixing of Au and Pd elements within the PVA-capped NPs (Fig. 7a). The PVP-capped NPs were also composed from homogenous Au-Pd elements (Fig. S9). In the elemental mapping line analysis of AuPd capped with DDAO, a higher concentration of Au atom can be seen around the center of the NPs (Fig. 7b) supporting low degree of AuPd alloying; *i.e.* Au-concentrated AuPd core@Pd-rich AuPd shell structure was expected in AuPd-DDAO NPs.

Combining all the studies of UV–vis, XRD, XPS and XAS (Au L_{III}-edge, Pd K- and L_{III}-edge) and STEM-EDS together, we can say that the electronic properties of Au and numbers of Au–Pd interfaces have been altered in the presence of different capping agents. The high electronegative Au species and more prominent alloying homogeneously were noticed for PVP and PVA capped catalysts, whereas moderately negative Au species owing to a small numbers of Au–Pd interactions in Au-concentrated AuPd core@Pd-rich AuPd shell structure was observed with AuPd-DDAO/HT. Choice of capping agent is crucial to control the electronic and geometric properties of metal nanoparticles [30,31,54].

4. Proposed reaction mechanism and role of capping agent

A suitable reaction pathway has been proposed based on the experimental facts combined with knowledge of literatures. In our previous paper, we confirmed a necessity of H_2O_2 and optimized its amount [32]. However, H_2O_2 completely disappeared during initial 20 min on all catalysts by a titration method accompanied with a fizzing from the reaction mixture. Therefore, the first step of the present HDO oxidation is proposed to be the catalytic decomposition of H_2O_2 into oxygen gas. It has been well-known that Au is able to decompose H_2O_2 by electron donation from Au to LUMO orbital of H_2O_2 [55]. To ensure the role of O_2 in the reaction, we performed the HDO oxidation under an O_2 flow without addition of H_2O_2 to afford 48% HCA yield with 75% HDO conversion [56]. In the case of the reaction with H_2O_2, the yield of HCA and HDO conversion were 81% and 87%, respectively (Table 1). These results confirmed a significant role of O_2 in the HDO oxidation: O_2 molecule from H_2O_2 is able to oxidize HDO by these AuPd-X/HT catalysts.

In the alcohol oxidation into carboxylic acid using O_2 and supported metal catalysts under high-pH conditions, O_2 is proposed to participate in the catalytic cycle not be dissociation to atomic oxygen but by regenerating hydroxide ions *via* the catalytic decomposition of a peroxide intermediate as follows [41].

$$O_2(ad) + H_2O(ad) \rightarrow OOH(ad) + HO(ad)$$

$$OOH(ad) + H_2O(ad) \rightarrow H_2O_2(ad) + HO(ad)$$

$$HO(ad) + e^- \rightarrow HO^-(ad)$$

The nature of surface hydroxide is probably influenced by the ability of metal to accommodate the excess negative charge to form AuO^- peroxo and/or AuO_2^- superoxo species as a key intermediate species [57]. The electronegativity of Au species attained in the presence of different capping agents explains the difference in catalytic behavior. The electronegativity of Au species is the order as PVA ≥ PVP > DDAO (*vide supra*). It is suggested that PVP-capped AuPd surface is highly active leading to very fast conversion of HDO into HCA, and HCA is readily converted to AA due to highly reactive OH species (low HCA selectivity). In case of DDAO-capped catalyst, the oxidizing ability of AuPd NPs is low to further transform HCA to AA, leading to the highest selectivity for HCA [58].

It is concluded that the role of capping agent is to control electronegativity of Au species by charge transfer from Pd and/or capping agent through alteration of AuPd NP morphology; *i.e.* the formation process of AuPd alloy is differed from the type of capping agent presents in preparation.

5. Catalytic oxidation of other aliphatic alcohols

After successful completion of the selective oxidation of C6 aliphatic diol (HDO), the catalytic system was further verified for selective oxidation of longer chain aliphatic diols such as C7 and C8 aliphatic diols.

The results clearly show that the system is acceptable for the selective synthesis of the mono-hydroxycarboxylic acids from 1,7-heptanediol and 1,8-octanediol with high selectivities (Fig. 8(1) and (2)). The reaction under the same condition oxidizes primary alcohol group selectively when both primary and secondary alcohol group were present; 1,2-hexanediol was selectively oxidized to 2-hydroxyhexanoic acid over AuPd-DDAO/HT in high yield and selectivity (Fig. 8 (3)) [59].

6. Conclusion

DDAO, PVP and PVA capped AuPd bimetallic NPs supported on HT (AuPd-X/HT) were prepared and their catalytic activities were explored for selective oxidation of long chain aliphatic diols in the presence of aqueous H_2O_2. High selectivity of mono-hydroxycarboxylic acid was achieved with reusable AuPd-DDAO/HT catalyst. The investigation on catalytic activity of supported AuPd bimetallic NPs capped with other capping agents such as PVP and PVA highlights the important role of capping agent for the selective oxidation. The characterization of differently capped catalysts concluded that the DDAO as capping agent could lead to synthesis of moderately negatively charged Au species in AuPd bimetallic NPs system with a few heterometallic Au—Pd bond. These particular sites of Au—Pd bond and specific $Au^{\delta-}$ species were found to play the key role in the production of mono-hydroxycarboxylic acids from long chain aliphatic diols with high selectivity.

Acknowledgements

We greatly appreciate Dr. Hemant Choudhary (JAIST, School of Materials Science) for his valuable suggestion of using DDAO as a capping agent. We also greatly thank Dr. Koichi Higashimine (JAIST, Center for Nano Materials and Technology) for his great supports in TEM and STEM-HAADF-EDS measurements. This work was partially supported by a Young Scientists (B) (No. 25820392) and Grant-in-Aid for Scientific Research (C) (No. 25420825) of the Ministry of Education, Culture, Sports, Science and Technology (MEXT), Japan. The authors also would like to appreciate to Prof. Keigo Kamata for his useful comments under the support of Collaborative Research Project of Materials and Structures Laboratory, Tokyo Institute of Technology (General C, H27-No. 23).

Please cite this article in press as: J. Tuteja, et al., Change in reactivity of differently capped AuPd bimetallic nanoparticle catalysts for selective oxidation of aliphatic diols to hydroxycarboxylic acids in basic aqueous solution, Catal. Today (2015), http://dx.doi.org/10.1016/j.cattod.2015.09.034

Appendix A. Supplementary data

Supplementary data associated with this article can be found, in the online version, at http://dx.doi.org/10.1016/j.cattod.2015.09.034.

References

[1] S. Carrettin, P. McMorn, P. Johnston, K. Griffin, G.J. Hutchings, Chem. Commun. 7 (2002) 696–697.
[2] X. Wang, G. Zhao, H. Zou, Y. Cao, Y. Zhang, R. Zhang, F. Zhang, M. Xian, Green Chem. 13 (2011) 2690–2695.
[3] G.L. Brett, P.J. Miedziak, Q. He, D.W. Knight, J.K. Edwards, S.H. Taylor, C.J. Kiely, G.J. Hutchings, ChemSusChem 10 (2013) 1952–1958.
[4] M.S. Ide, R.J. Davis, J. Catal. 308 (2013) 50–59.
[5] D. Tongsakul, S. Nishimura, K. Ebitani, ACS Catal. 3 (2013) 2199–2207.
[6] K. Zaw, M. Lautens, P.M. Henry, Organometallics 2 (1983) 197–199.
[7] D.G. Lee, U.A. Spitzer, J. Org. Chem. 35 (1970) 3589–3590.
[8] P.V. Prabhakaran, S. Venkatachalam, K.N. Ninan, Eur. Polym. J. 35 (1999) 1743–1746.
[9] J. Muzart, Tetrahedron 59 (2003) 5789–5816.
[10] R.A. Sheldon, J.K. Kochi, Metal-Catalyzed Oxidations of Organic Compounds, Academic Press, New York, 1981.
[11] G. Tojo, M. Fernandez, Oxidations of Alcohols to Aldehydes and Ketones, Springer, New York, 2006.
[12] M.C. Daniel, D. Astruc, Chem. Rev. 104 (2004) 293–346.
[13] A. Roucoux, J. Schulz, H. Patin, Chem. Rev. 102 (2002) 3757–3778.
[14] E.C. Dreaden, A.M. Alkilany, X. Huang, C.J. Murphy, M.A. El-Sayed, Chem. Soc. Rev. 41 (2012) 2740–2779.
[15] R. Ferrando, J. Jellinek, R.L. Johnston, Chem. Rev. 108 (2008) 845–910.
[16] M. Sankar, N. Dimitratos, P.J. Miedziak, P.P. Wells, K.J. Christopher, G.J. Hutchings, Chem. Soc. Rev. 41 (2012) 8099–8139.
[17] H.-L. Jiang, Q. Xu, J. Mater. Chem. 21 (2011) 13705–13725.
[18] A.K. Singh, Q. Xu, ChemCatChem 5 (2013) 652–676.
[19] D.I. Enache, J.K. Edwards, P. Landon, B. Solsona-Espriu, A.F. Carley, A.A. Herzing, M. Watanabe, C.J. Kiely, D.W. Knight, G.J. Hutchings, Science 311 (2006) 362–365.
[20] D. Martin Alonso, S.G. Wettsteina, J.A. Dumesic, Chem. Soc. Rev. 41 (2012) 8075–8098.
[21] H. Zhang, N. Toshima, Catal. Sci. Technol. 3 (2013) 268–278.
[22] N. Dimitratos, J.A. Lopez-Sanchez, G.J. Hutchings, Chem. Sci. 3 (2012) 20–44.
[23] S.E. Davis, M.S. Ide, R.J. Davis, Green Chem. 15 (2013) 17–45.
[24] F. Maroun, F. Ozanam, O.M. Magnussen, R.J. Behm, Science 293 (2001) 1811–1814.
[25] M.S. Chen, D. Kumar, C.W. Yi, D.W. Goodman, Science 310 (2005) 291–293.
[26] T. Wei, J. Wang, D.W. Goodman, J. Phys. Chem. C 111 (2007) 8781–8788.
[27] J.K. Norskov, T. Bligaard, J. Rossmeisl, C.H. Christensen, Nat. Chem. 1 (2009) 37–46.
[28] N. Toshima, T. Yonezawa, N. J. Chem. 22 (1998) 1179–1201.
[29] C.-H. Chen, L.S. Sarma, J.-M. Chen, S.-C. Shih, G.-R. Wang, D.-G. Liu, M.-T. Tang, J.-F. Lee, B.-J. Hwang, ACS Nano 1 (2007) 114–125.
[30] S.M. Humphrey, M.E. Grass, S.E. Habas, K. Niesz, G.A. Somorjai, T.D. Tilley, Nano Lett. 7 (2007) 785–790.
[31] H. Choudhary, S. Nishimura, K. Ebitani, ChemCatChem 7 (2015) 2361–2369.
[32] J. Tuteja, S. Nishimura, H. Choudhary, K. Ebitani, ChemSusChem 8 (2015) 1862–1866.
[33] G.C. Bond, D.T. Thompson, Catal. Rev. Sci. Eng. 41 (1999) 319–388.
[34] F. Porta, L. Prati, M. Rossi, S. Coluccia, G. Martra, Catal. Today 61 (2000) 165–172.
[35] D. Zhao, Y.H. Wang, B.Q. Xu, J. Phys. Chem. C 113 (2009) 20903–20911.
[36] M. Turner, V.B. Golovko, O.P. Vaughan, P. Abdulkin, A. Berenguer-Murcia, M.S. Tikhov, B.F. Johnson, R.M. Lambert, Nature 454 (2008) 981–983.
[37] N. Shalkevich, W. Escher, T. Bu, B. Michel, L. Si-Ahmed, D. Poulikakos, Langmuir 26 (2010) 663–670.
[38] W. Chen, S.W. Chen, Angew. Chem. Int. Ed. 48 (2009) 4386–4389.
[39] S. Nishimura, Y. Yakita, M. Katayama, K. Higashimine, K. Ebitani, Catal. Sci. Technol. 3 (2013) 351–359.
[40] M. Mohammad, S. Nishimura, K. Ebitani, AIP Conf. Proc. 1549 (2015) 58–66.
[41] B.N. Zope, D. Hibbitts, M. Neurock, R.J. Davis, Science 330 (2010) 74–78.
[42] S. Link, M.A. El-Sayed, J. Phys. Chem. B 103 (1999) 4212–4217.
[43] H. Yang, D. Tang, X. Lu, Y. Yuan, J. Phys. Chem. C 113 (2009) 8186–8193.
[44] G. Zhan, J. Huang, M. Du, I. Abdul-Rauf, Y. Ma, Q. Li, Mater. Lett. 65 (2011) 2989–2991.
[45] S. Nishimura, N. Ikeda, K. Ebitani, Catal. Today 232 (2014) 89–98.
[46] Y.W. Lee, N.H. Kim, K.Y. Lee, K. Kwon, M. Kim, S.W. Han, J. Phys. Chem. C 112 (2008) 6717–6722.
[47] C.-W. Yi, K. Luo, T. Wei, D.W. Goodman, J. Phys. Chem. B 109 (2005) 18535–18540.
[48] J. Xu, T. White, P. Li, C. He, J. Yu, W. Yuan, Y.-F. Han, J. Am. Chem. Soc. 132 (2010) 10398–10406.
[49] A. Murugadoss, K. Okumura, H. Sakurai, J. Phys. Chem. C 116 (2012) 26776–26783.
[50] F. Liu, D. Wechsler, P. Zhang, Chem. Phys. Lett. 461 (2008) 254–259.
[51] T. Balcha, J.R. Strobl, C. Fowler, P. Dash, R.W.J. Scott, ACS Catal. 1 (2011) 425–436.
[52] S. Marx, A. Baiker, J. Phys. Chem. C 113 (2009) 6191–6201.
[53] R.J. Davis, M. Boudart, J. Phys. Chem. 98 (1994) 5471–5477.
[54] D. Tongsakul, S. Nishimura, K. Ebitani, J. Phys. Chem. C 118 (2014) 11723–11730.
[55] A. Thetford, G.J. Hutchings, S.H. Taylor, D.J. Willock, Proc. R. Soc. A 467 (2011) 1885–1899.
[56] The reaction under an N2 flow scarcely gave HCA.
[57] M. Okumura, Y. Kitagawa, M. Haruta, K. Yamaguchi, Chem. Phys. Lett. 346 (2001) 163–168.
[58] We found that an addition of small amount of melatonin (0.05 mmol), known as water-soluble hydroxyl radical scavenger, drastically impeded the HDO oxidation by AuPd-DDAO/HT catalyst. At the present, however, we could not infer whether this oxidation proceeds via radical or non-radical pathway because of a strong coordination ability of melatonin molecule on metal surface.
[59] In addition, the present catalytic system is also able to oxidize non-activated primary alcohol (1-hexanol) to the corresponding carboxylic acid (hexanoic acid).

Please cite this article in press as: J. Tuteja, et al., Change in reactivity of differently capped AuPd bimetallic nanoparticle catalysts for selective oxidation of aliphatic diols to hydroxycarboxylic acids in basic aqueous solution, Catal. Today (2015), http://dx.doi.org/10.1016/j.cattod.2015.09.034